JOURNAL OF MATERIALS SCIENCE 28 (1993) 5275–5279

Processing maps for hot working of Cu–Ni–Zn alloys

Part II α–β *nickel silver*

D. PADMAVARDHANI, Y. V. R. K. PRASAD
Department of Metallurgy, Indian Institute of Science, Bangalore 560012, India

The constitutive behaviour of α–β nickel silver in the temperature range 600–850 °C and strain-rate range 0.001–100 s^{-1} was characterized with the help of a processing map generated on the principles of the dynamic materials model. On the basis of the flow-stress data, processing maps showing the variation of the efficiency of power dissipation (given by $[2m/(m+1)]$, where m is the strain-rate sensitivity) with temperature and strain rate were obtained. α–β nickel silver exhibits a single domain at temperatures greater than 700 °C and at strain rates lower than 1 s^{-1} with a maximum efficiency of power dissipation of about 42% occurring at about 850 °C and at 0.1 s^{-1}. In the domain, the α phase undergoes dynamic recrystallization and controls the deformation of the alloy, while the β phase deforms superplastically. Optimum conditions for the processing of α–β nickel silver are 850 °C and 0.1 s^{-1}. The material undergoes unstable flow at strain rates of 10 and 100 s^{-1} and in the temperature range 600–750 °C, manifestated in the form of adiabatic shear bands.

1. Introduction

Many engineering alloys are two-phase alloys and these are generally shaped into components by hot working. For optimization of hot workability and control of microstructure, a knowledge of the constitutive behaviour of the material under hot-working conditions is essential. From this view point, two-phase alloys are complex. For example, in these alloys, it is not understood how each phase deforms and which one of the phases controls the hot deformation of the alloy. Recently, an attempt has been made to understand the mechanisms of hot deformation in two-phase alloys by taking α–β brass as an example [1]. The constitutive behaviour of the individual phases was established, on the basis of which the mechanisms of hot deformation in the two-phase alloy were examined. It was shown that in the two-phase alloy, each phase deforms according to its individual constitutive behaviour and the harder of the two phases controls the deformation of the alloy. In α–β brass, the α phase undergoes dynamic recrystallization (DRX) and controls the hot deformation of the alloy while the β phase deforms superplastically. Therefore, it is expected that any change in the constitutive behaviour of the controlling phase alters the hot-deformation behaviour of the two-phase alloy.

The aim of the present investigation was to examine whether the two-phase alloy responds to the changes in the constitutive behaviour of the controlling α phase. Nickel was chosen as the alloying element because it stabilizes and partitions to α. In addition, the constitutive behaviour of α is altered [2] by the addition of nickel as it increases the activation energy for diffusion [3]. Earlier, many investigations were carried out on microduplex nickel silvers and superplasticity in this alloy was established [4–8]. Cavitation, cavity growth and sintering during the superplastic deformation were studied extensively. The hot workability of two-phase nickel silvers of different compositions was assessed in a qualitative way [9]. These alloys have good hot workability but their cold workability is poor. The addition of 4 %–9 % Mn was reported to improve the general workability of two-phase Cu–Ni–Zn alloys [10]. Most of the earlier investigations were carried out at low strain rates. Therefore, it was proposed to study the hot-deformation behaviour of two-phase nickel silver over a wide range of strain rates and temperatures. For this study, the approach of characterizing the hot-deformation behaviour using processing maps was adopted. The basis for this approach is the dynamic materials model (DMM) developed by Prasad *et al.* [11] and reviewed recently by Gegel *et al.* [12] and Alexander [13]. This model was discussed in detail earlier [2]. The efficiency of power dissipation is plotted as a function of temperature and strain rate in the form of a three-dimensional processing map with hills and valleys. For easy perception, it can be viewed on a two-dimensional temperature–strain rate plane with iso-efficiency contours. The processing map shows deterministic domains corresponding to various micromechanisms.

The regimes of microstructural instabilities are evaluated using the criterion developed by Kumar [14] and Prasad [15] on the basis of Ziegler's principle of maximum rate of entropy production [16]. It

0022–2461

was shown that instabilities in microstructure will occur if

$$\partial \ln [m/(m+1)]/(\partial \ln \dot{\varepsilon}) + m < 0 \quad (1)$$

The left-hand side of Equation 1 is denoted by $\xi(\dot{\varepsilon})$, the variation of which is plotted as a function of temperature and strain rate to obtain an instability map.

2. Experimental procedure

α–β nickel silver with 42.7% Zn, 12.4% Ni and the balance copper was used in this investigation. The material was used in the as-cast condition. Details of the experimental procedure were given elsewhere [2]. In brief, cylindrical specimens of 10 mm diameter and 15 mm height were used for the compression testing of the alloy. The temperature range employed in the study was 600–850 °C and the strain-rate range was 0.001–100 s^{-1}. In each case, the specimens were compressed to about half their height in the computer-controlled servohydraulic testing machine (Dartec, UK). The deformed specimens were water quenched and examined using standard metallographic techniques. Tensile testing of the samples was carried out in the temperature range 650–850 °C and at a strain rate of 0.1 s^{-1} to establish the ductility values.

3. Results and discussion

3.1. Stress–strain curves

Typical true stress–true plastic strain curves recorded on α–β nickel silver are shown in Fig. 1a and b at temperatures of 650 and 850 °C and at different strain rates. The following features may be observed.

1. At 650 °C, at strain rates of 0.001 and 0.01 s^{-1}, steady-state behaviour is observed at higher strains. At 0.1 and 1 s^{-1}, slight flow-softening is observed. At higher strain rates, oscillations and flow-softening is seen (Fig 1a).

2. The oscillations at higher strain rates persisted at high temperatures (Fig. 1b).

3. At high temperatures (850 °C, Fig. 1b), at strain rates lower than 1 s^{-1}, steady-state behaviour is observed (Fig. 1b).

The flow-stress data corrected for the adiabatic temperature rise are shown in Table I for α–β nickel silver.

3.2. Processing maps

The processing map of α–β nickel silver is shown in Fig. 2 for a strain of 0.5. The maps obtained at other strains are essentially similar to that in Fig. 2. The map exhibits a single domain at strain rates lower than 1 s^{-1} and at temperatures greater than 700 °C with a maximum efficiency of power dissipation of 42 % occurring at about 850 °C and 0.1 s^{-1}. In contrast to the map for α–β brass wherein a maximum efficiency of 54 % was observed, the peak efficiency in the case of α–β nickel silver is only 42 %. The strain rate for maximum efficiency in the present case has risen by two orders of magnitude (from 0.001 s^{-1} in the case of two-phase Cu–Zn alloy, to 0.1 s^{-1} with the addition of nickel). Earlier it was shown that during the hot deformation of the two-phase α–β brass, each of the phases deforms according to its constitutive behaviour (the α phase undergoes DRX while the β phase deforms superplastically) and the hot deformation of the alloy is controlled by the α phase. Therefore, any change in the constitutive behaviour of α phase should be reflected in the α–β alloy. Nickel partitions to α and does not alter the constitutive behaviour of β. Nickel increases the activation energy for diffusion, results in increased strain rate for DRX and lowers the maximum efficiency of power dissipation [2]. As α is the controlling phase in the case of α–β alloy, the strain rate for maximum efficiency has risen by two orders of magnitude and the maximum efficiency has fallen to 42 % with the addition of nickel. The processing map for α–β nickel silver is strikingly similar to that of α nickel silver. Therefore, in the case of α–β nickel silver, the α phase undergoes DRX and controls the hot deformation of the alloy.

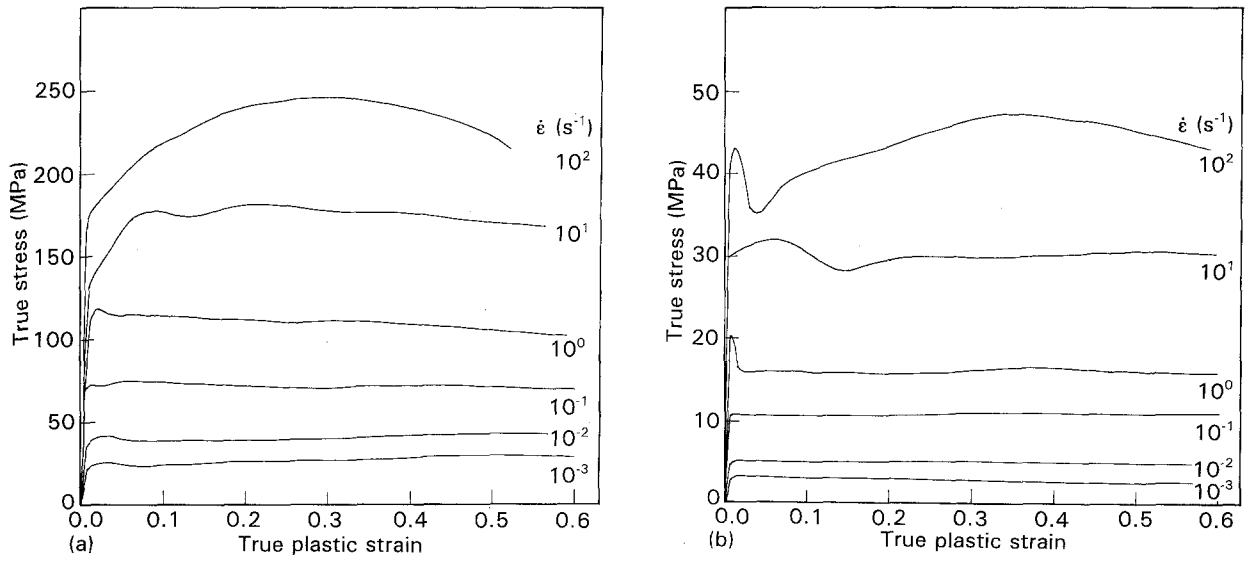

Figure 1 True stress–true plastic strain curves for α–β nickel silver (a) 700 °C and (b) 950 °C, at various strain rates.

TABLE I Flow-stress values of α–β nickel silver at different strain rates and temperatures for various strains (corrected for adiabatic temperature rise)

Strain	Strain rate (s^{-1})	Flow stress (MPa)					
		600 °C	650 °C	700 °C	750 °C	800 °C	850 °C
0.1	0.001	36.8	25.0	14.1	9.8	5.0	2.8
	0.010	61.4	38.8	25.3	12.4	9.1	4.8
	0.100	113.8	74.1	40.1	23.2	14.1	10.5
	1.000	220.5	129.9	76.4	46.0	26.7	16.0
	10.000	241.8	193.6	133.6	81.9	59.0	32.1
	100.000	221.6	219.5	172.8	111.9	71.6	42.7
0.2	0.001	38.9	26.0	15.3	10.2	5.1	2.8
	0.010	62.0	39.6	25.9	13.5	9.3	4.8
	0.100	113.1	71.5	39.4	23.7	14.5	10.7
	1.000	228.0	127.9	73.8	45.7	26.8	15.8
	10.000	327.2	213.0	133.5	80.8	56.6	31.2
	100.000	327.7	262.9	190.1	123.2	78.9	45.9
0.3	0.001	41.3	26.9	15.7	9.6	4.9	2.6
	0.010	63.9	40.5	26.2	13.9	9.3	5.1
	0.100	112.5	71.9	39.9	24.6	14.9	11.2
	1.000	219.9	125.5	72.8	45.6	27.3	16.2
	10.000	332.2	210.9	131.1	79.8	56.2	31.3
	100.000	398.1	282.5	197.5	130.9	83.5	49.4
0.4	0.001	42.3	27.7	15.6	9.0	4.7	2.7
	0.010	65.7	41.9	26.5	14.4	9.4	4.9
	0.100	113.3	72.2	40.4	25.3	15.2	11.1
	1.000	212.4	121.9	72.6	45.9	27.9	16.3
	10.000	326.9	208.0	130.8	82.1	57.3	31.9
	100.000	411.4	279.8	195.8	132.0	85.0	49.6
0.5	0.001	43.3	28.0	15.1	8.5	4.4	2.7
	0.010	66.0	42.8	26.4	14.4	8.9	4.8
	0.100	112.7	71.2	40.6	25.3	15.0	10.9
	1.000	204.7	118.0	70.8	46.1	28.0	16.0
	10.000	313.5	201.0	127.8	82.8	56.7	31.9
	100.000	381.1	258.6	186.1	127.5	82.6	47.8

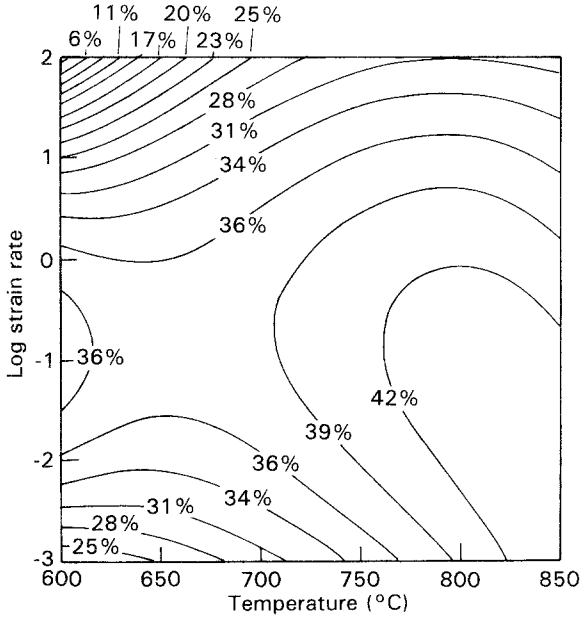

Figure 2 Contour map showing iso-efficiency contours in the strain rate–temperature plane for α–β nickel silver at a strain of 0.5. The numbers indicate the efficiency of power dissipation.

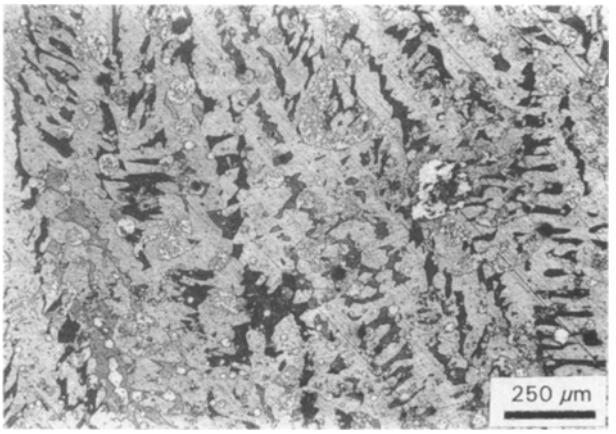

Figure 3 Initial microstructure of α–β nickel silver showing dendrites typical of as-cast material.

The initial microstructure is given in Fig. 3 which shows dendritic structure typical of as-cast material. The microstructures of the sample deformed in the domain (e.g. 850 °C and 0.01 s^{-1}) are shown in Fig. 4a and b at low and high magnification, respectively. In comparison with the initial microstructure (Fig. 3), a large-scale reconstitution of the α phase morphology is seen. The as-cast dendritic structure is totally broken, globularization of α phase occurred and certain waviness in the α phase boundaries is seen (Fig. 4). A similar feature was also observed in the case of α–β brass [1]. This confirms that the α phase has undergone dynamic recrystallization. In contrast, the

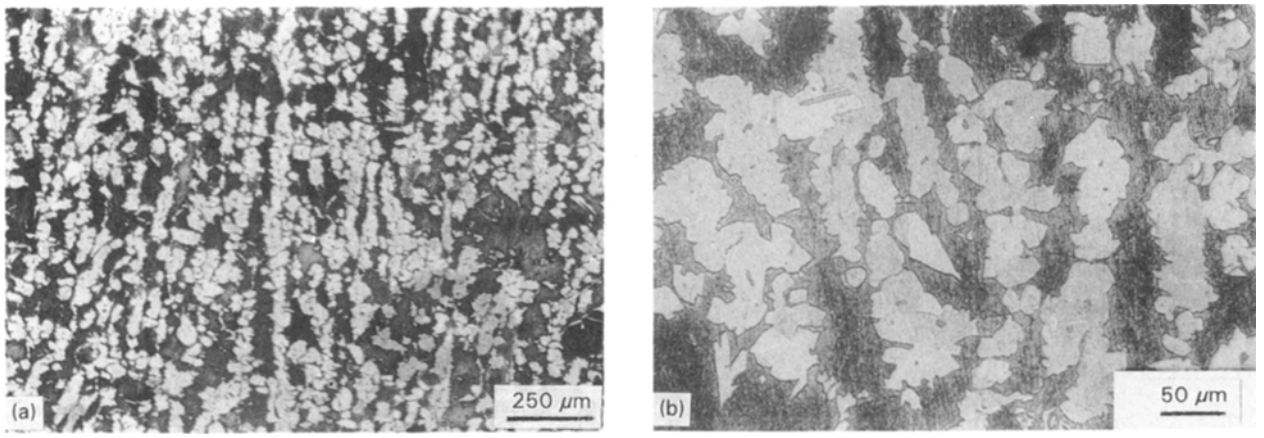

Figure 4 (a, b) Microstructure of α–β nickel silver specimen deformed at 850 °C and 0.01 s^{-1} showing globularized α phase, at low and high magnification, respectively.

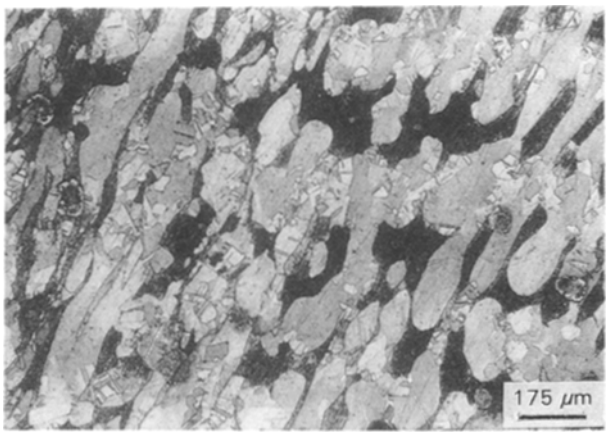

Figure 5 Microstructure of α–β nickel silver specimen deformed at 700 °C and 0.01 s^{-1}.

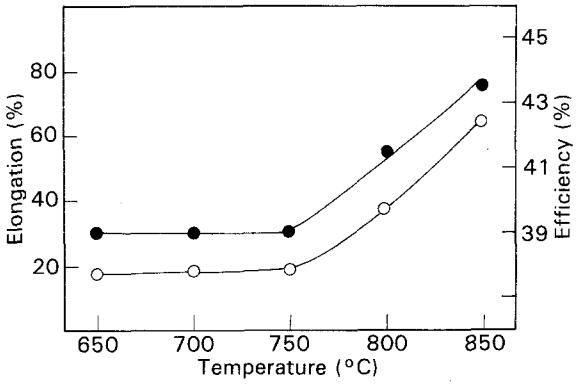

Figure 6 Variation of the (○) tensile ductility and (●) the efficiency of power dissipation for α–β nickel silver with temperature.

microstructure of the specimen deformed under conditions outside the domain (e.g. 700 °C and 0.01 s^{-1}) shows static recrystallization following dynamic recovery (Fig. 5).

The variation of the tensile ductility and the efficiency of power dissipation as a function of temperature in the domain are shown in Fig. 6. The two variations

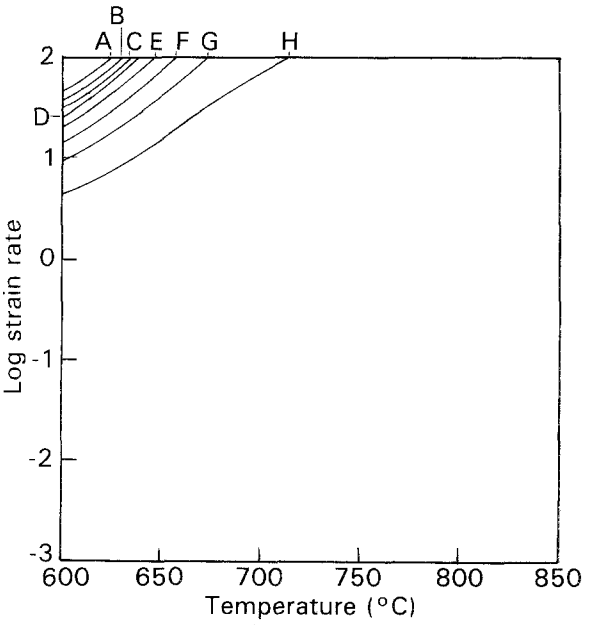

Figure 7 Instability map showing contours of instability parameter ξ(ε̇) in the strain rate–temperature plane for α–β nickel silver at a strain of 0.5. Instability is predicted when ξ(ε̇) is negative: ξ(ε̇): (A) – 0.88, (B) – 0.75, (C) – 0.63, (D) – 0.50, (E) – 0.38, (F) – 0.25, (G) – 0.13, (H) – 0.00.

are identical. On the basis of the map, the optimum conditions for hot working this alloy are 850 °C and 0.1 s^{-1}. These match those generally employed for the hot working of α–β nickel silver [17].

3.3. Instability maps

The instability map developed on the basis of the continuum criterion given by Equation 1, at a strain of 0.5 is shown in Fig. 7. Instability is predicted in the temperature range 600–750 °C and at strain rates of 10 and 100 s^{-1}. It is in this regime that the stress–strain curves exhibit oscillations. The microstructure corresponding to the specimens deformed in this regime are shown in Fig. 8a–c which show that the instability is manifested in the form of adiabatic shear bands. These instabilities disappear when the strain rate is reduced

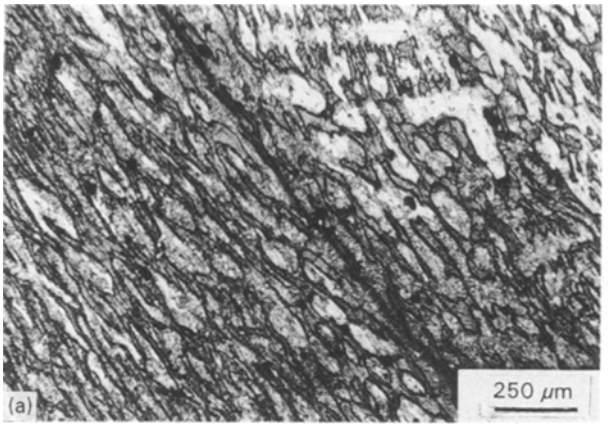

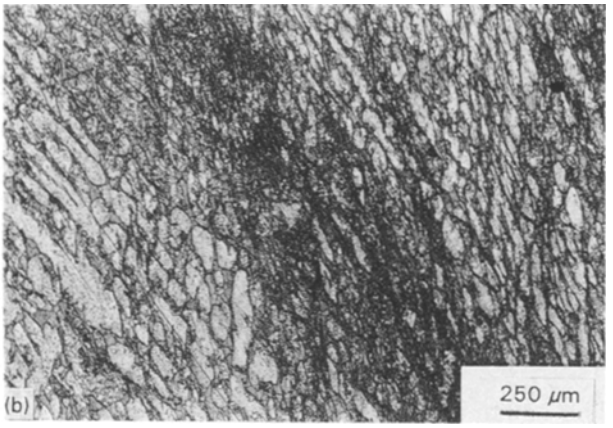

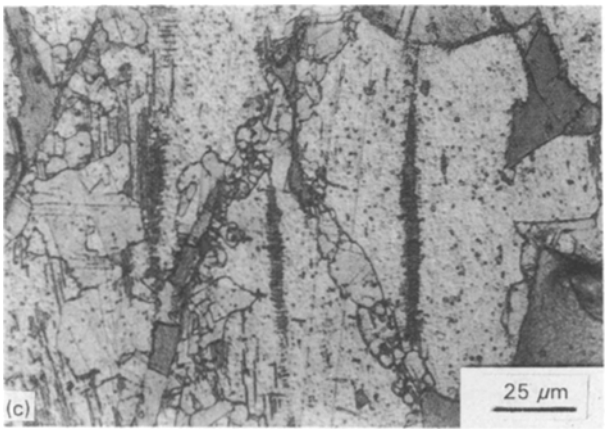

Figure 8 (a) Microstructure of the α–β nickel silver specimen deformed at 600 °C and at (a) $100\,s^{-1}$ (b) $10\,s^{-1}$ (instability regions) revealing adiabatic shear bands and at (c) $10\,s^{-1}$ (instability region), revealing adiabatic shear bands in the α phase.

or when the temperature is increased. The instability is more intense in the specimen deformed at $100\,s^{-1}$ (Fig. 8a) than when compared with that at $10\,s^{-1}$ (Fig. 8b). At lower strain rate, diffuse banding has occurred (Fig. 6b). The microstructure of the specimen deformed at 600 °C and $10\,s^{-1}$ exhibited adiabatic shear bands in the α phase (Fig. 6c) which are similar to those observed in the case of α nickel silver [2].

4. Conclusions

The hot deformation behaviour of α nickel silver was studied in the temperature range 600–850 °C and strain-rate range $0.001–100\,s^{-1}$. The following conclusions are drawn.

1. α–β nickel silver exhibits a domain at temperatures greater than 750 °C and at strain rates lower than $1\,s^{-1}$.

2. The maximum efficiency of power dissipation in the domain is 42 % and occurs at about 850 °C and at a strain rate of $0.1\,s^{-1}$.

3. In the domain the α phase undergoes dynamic recrystallization while the β phase deforms superplastically.

4. The hot deformation of the alloy is controlled by the α phase.

5. The optimum conditions for processing of the α–β nickel silver are 850 °C and $0.1\,s^{-1}$.

6. The material undergoes unstable flow in the temperature range 600–750 °C and at strain rates of 10 and $100\,s^{-1}$ as predicted by the instability criterion. The manifestation is in the form of adiabatic shear bands.

References

1. D. PADMAVARDHANI and Y. V. R. K. PRASAD, *Metall. Trans.* **22A** (1991) 2996.
2. *Idem, J. Mater. Sci.* **28** (1993) 0000
3. K. J. ANUSAVICE and R. T. DEHOFF, *Metall. Trans.* **3A** (1972) 1279.
4. R. D. SCHELLENG and G. H. REYNOLDS, *ibid.* **4A** (1973) 2199.
5. D. W. LIVESEY and N. RIDLEY, *ibid.* **9A** (1978) 519.
6. *Idem, ibid.* **13A** (1982) 1619.
7. D. W. LIVESEY and N. RIDLEY, *Metall. Sci.* **16** (1982) 563.
8. *Idem, J. Mater. Sci.* **19** (1984) 3602.
9. M. COOK, *J. Inst. Metals* **66** (1) (1938) 139.
10. D. M. WARD and B. J. HELLIWELL, *ibid.* **98** (1970) 98.
11. Y. V. R. K. PRASAD, H. L. GEGEL, S. M. DORAIVELU, J. C. MALAS, J. T. MORGAN, K. A. LARK and D. R. BARKER, *Metall. Trans.* **15A** (1984) 1883.
12. H. L. GEGEL, J. C. MALAS, S. M. DORAIVELU, V. A. SHENDE, in "Metals Handbook", 9th Edn, Vol. 14 (ASM International, Metals Park, OH, 1987) p. 417.
13. J. M. ALEXANDER, in "Modelling of Hot Deformation of Steels", edited by J. G. Lenard (Springer, Berlin, 1989) p. 101.
14. A. K. S. KALYAN KUMAR, MSc (Engng) thesis, Indian Institute of Science, Bangalore, India (1987).
15. Y. V. R. K. PRASAD, *Indian J. Tech.* **28** (1990) 435.
16. H. ZIEGLER, in "Progress in Solid Mechanics", edited by I. N. Sneddon and R. Hill (North-Holland, Amsterdam, 1963) p. 93.
17. K. LAUE and H. STENGER, in "Extrusion" (ASM, Metals Park, OH, 1981) p. 109.

Received 25 March 1992
and accepted 24 February 1993